Measurement of Gas Flow and Oxygenation in Small Animal Lungs Using Hyperpolarized Gas

S. J. Kadlecek[1], P. Mongkolwisetwara[1], K. Emami[1], M. Ishii[2], J. Zhu[3], E. Chia[1], J. M. Woodburn[1], and R. R. Rizi[1]
[1]Department of Radiology, University of Pennsylvania, Philadelphia, PA, United States, [2]Department of Otolaryngology, Johns Hopkins University, Baltimore, MD, United States, [3]Department of Surgery, University of Pennsylvania, Philadelphia, PA, United States

Introduction: In contrast to most proton MRI, T_1 measurements of hyperpolarized gas in the lung are particularly straightforward to interpret. This is because the dominant source of relaxation arises from a single source: collisions with paramagnetic oxygen molecules. Several investigators have used this property to determine the regional oxygen concentrations that have been shown to correspond well to physiologically expected values. However, measurements in small animals are less straightforward due to the animals' rapid uptake of oxygen in the lung and their inability to tolerate extended breath-holds without physiological change. We have found that T_1 measurements consisting of only a few seconds can suffer on the one hand from noise when constraining the ~10-20-second true T_1, and on the other hand from gas flow and redistribution during the early moments of a short breath-hold. By introducing signal-averaging over multiple breaths, as well as two additional parameters sensitive to gas flow, we increase the accuracy of oxygen measurements and learn additional details about ventilation and air-trapping.

Materials and Methods: Fourteen male Sprague-Dawley rats between 300 and 370 g were utilized for this technique development as part of a larger study of the effect of disease states on pulmonary oxygen tension. Seven animals were imaged naive, and seven before and after the following treatments: two animals received lung-volume reduction surgery, two were sham-treated for LVRS (surgery but no lung volume removal), and three were subjected to bleomycin instillation (a model of acute respiratory distress syndrome). Animals were steadily ventilated with a 5:1 He:O_2 mixture at 60 BPM and an I:E ratio of 1:2, with the exception of a 4-5 second breath-hold on every tenth breath. A series of transverse slice images (GRE, MS=64x64, TR/TE=2.1/1.2 ms) was acquired, one per breath-hold. The slice location and delay after the beginning of the breath-hold were varied for a total of three slices × five delays = fifteen images. The sequence was then repeated until the supply of hyperpolarized gas was depleted, typically after approximately sixty images. Each imaging sequence required approximately fifteen minutes to complete. This process is illustrated more fully in **Fig. 1.** The resulting images were first adjusted for polarization loss in the gas reservoir (extracted reservoir T_1s varied from 40 minutes to over 1 hour). Images corresponding to the same slice/delay combination were then averaged together and fit to the model of eq. 1: the four parameters, corresponding to initial signal intensity *S(0)*, characteristic oxygen-induced decay rate time τ_{O2}, fractional flow volume f_r and characteristic gas redistribution time τ_r were allowed to vary independently except for the requirement that $\tau_{O2} < \tau_r$. Note that except in cases of extreme pathology, the two timescales are well separated (τ_{O2} ~ 10-20 sec, τ_r ~ 0.5-1s) so this requirement protects against misassignment of the parameters. Apparent P_AO_2 is derived from τ_{O2} and a measured scaling constant of 2.62 bar-s. Because of complete gas refresh between images, the flip-angle does not appear as a fit parameter. The pixel-by-pixel fit was performed with custom MATLAB (Mathworks, Natick, MA) programs developed in-house.

$$S(t) = S(0)\left(1 - f_r e^{-t/\tau_r}\right)e^{-t/\tau_{O2}} \qquad \text{(eq 1.)}$$

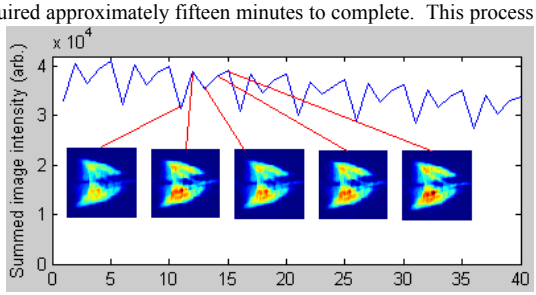

Figure 1: Sample time-series of summed image intensities for a single slice imaged forty times with intra-breathhold delays of (4, 0.5, 2, 1, 0.25, 4, 0.5,…) seconds. Images with identical delay are summed in the inset figures. Note the observable T_1 signal attenuation in the first and third images.

Results and Discussion: Several features of the fit image series are notable and common to all series. First, short-time gas redistribution is dominated by flow out of the airways and into the lung periphery. In previous attempts to measure P_AO_2 in small animals, characteristic errors were introduced by interpreting this flow as T_1 relaxation, despite its differing time-scale. **Fig. 2** illustrates this feature. Second, a focal region of apparent elevated oxygen is universally seen in the left lung, which is likely an artefact due to increased air movement near the beating heart (**Fig. 3**). Third, we found that focal abnormalities in each parameter are usually separable, e.g., they appear chiefly in maps of one image parameter, suggesting that the disparate time-scales allow for a stable fit. However, in several instances, highly correlated parameter maps were seen; often, the correlated abnormalities could be interpreted as mild or reversible ventilation defects that filled in slowly over the course of the few-second breath-hold. It is notable that these defects are often poorly visualized or invisible in the signal intensity maps. We also note that focal abnormalities were observed in healthy animals, suggesting the onset of atelectasis due to animal positioning, anaesthesia or ventilation (explored in another abstract). An example of this is illustrated in **Fig. 4**. With respect to the comparison between control and disease model animals, we observed no consistent change in the average value of any fit parameter, perhaps due to the failure to identify and ameliorate reversible focal atelectatic change in control animals.

Conclusion and Future Directions: We have performed initial investigations of the separation of flow-induced temporal signal changes during breath-holds from those truly indicative of oxygen-induced T_1. The technique shows promise for highlighting patterns of airflow, including that from airways to the periphery, resulting in highly conspicuous airways. It also highlights focal regions of abnormal airflow time-constants, likely indicative of a condition analogous to air-trapping. Finally, we find that apparent physiological abnormalities are often conspicuous even if not well visualized using signal-intensity or apparent diffusion coefficient maps.

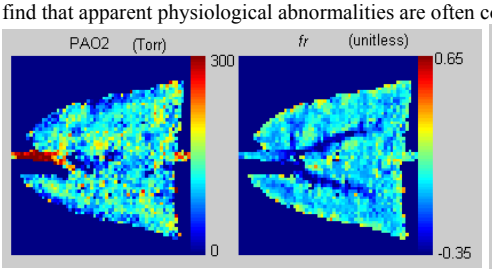

Figure 2: Derived characteristics of flow and oxygen tension in the healthy rat lung (fit parameters P_AO_2 and f_r.) which represents the flow direction. Note that the f_r map describes gas leaving the airways, which are highly conspicuous. Failure to incorporate the modelling of gas flow would result in an artificially elevated derived P_AO_2. Expansion of the lung during the breath-hold (highlighted edges) is also incorporated into this parameter, removing an additional artefact from P_AO_2.

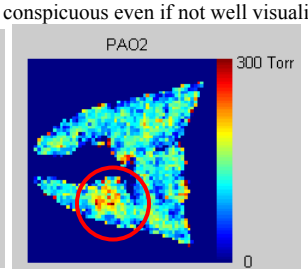

Figure 3: Apparent P_AO_2 as derived from τ_{O2}. The demonstrated level of uniformity is typical of both the healthy and disease-model lung; elevated oxygen tension in the airways and an apparent motion-induced artefact due to increased flow near the heart (shown) are universal. Often other, usually peripheral, nonuniformities are seen as well.

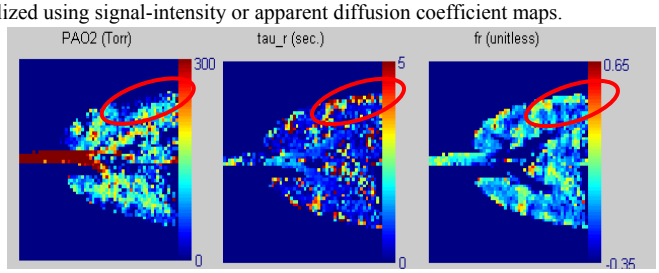

Figure 4: P_AO_2/airflow imaging highlights regions of reduced ventilation (analogous to air trapping) as simultaneously reduced P_AO_2 (left), net positive airflow (middle) at breath-hold, and slow filling rate (right). Focal regions appearing throughout the periphery of the lung suggest the onset of atelectasis.